Research Square

Preprints are preliminary reports that have not undergone peer review.
They should not be considered conclusive, used to inform clinical practice,
or referenced by the media as validated information.

Entrainment of Chaotic Oscillations in a Colonial Tunicate.

Michael W. Konrad (mwkonrad@scienceisart.com)
Science Is Art, 3 S 40 Dock

Research Article

Keywords: Tunicate, Tunicata, Botrylloides, Ampullae, Heart, Chaotic, Entrainment

Posted Date: March 11th, 2022

DOI: https://doi.org/10.21203/rs.3.rs-655370/v2

License: This work is licensed under a Creative Commons Attribution 4.0 International License.
Read Full License

Introduction

Ascidian colonial tunicates contain two distinct but connected blood compartments. In each zooid blood is circulated by a peristaltic heart. This circulation system is connected to a common or colonial network. Typically, two vessels extend from each zooid radially to a vessel ring and extensions from the ring extend to terminate in bulbs or ampullae, approximately evenly distributed around the edge of the colony. These ampullae expand and contract about every 100 seconds, mostly in synchrony. Bancroft (Bancroft 1899), more than 100 years ago observed blood flow in groups of ampullae surgically removed from colonies and deduced they were still contracting. Thus, while ampullae and peristaltic hearts are connected, they are not dependent on each other to pump blood.

Botrylloides viocella is the tunicate species studied in this report. The very similar *Botryllus schlosseri* is the subject of many more publications. The major difference between the species is the pattern of zooid clustering. Large colonies of *B. viocella* contain long rows of zooids, with each zooid having an exposed oral siphon but expelling water from large common openings that appear in apparently random locations in the colonial tunic. In *B. schlosseri* colonies are made up of many star-like groups of up to 12 zooids, again each having an exposed oral siphon but sharing a common cloacal opening at the center of the cluster. The number of ampullae in colonies immediately after the founding "tadpole" has attached to a substrate varies between species, in *B. viocella* there are between 30 to 40.

The present study is the first comprehensive quantitative description of the sizes and shapes of components of the colony recorded as a function of time. However, it will be most useful if it can be integrated with and extend our present understanding the biology of the tunicate. The recent review "The biology of the extracorporeal vasculature of *Botryllus schlosseri* " (Rodriguez et al.

2019) is thus very relevant. The major immune role of the vasculature has been reviewed by Rosental et al. (Rosental et al. 2018), ontology of the anatomy and development of B. Schlosseri is described in (Manni et al. 2014), culture and reproduction is reviewed by Gasparini et al. (Gasparini et al. 2014), angiogenesis of the vasculature is reviewed by Tiozzo et al. (**Tiozzo** et al. 2008), and the review by Manni et al. (Manni et al. 2007) is also very useful.

Materials & Methods

Collection and maintenance of tunicates

Tunicate colonies were collected from the sides of floating docks in Sausalito, California and transferred to an aerated aquarium. Tadpoles released from these colonies during the next 24 to 48 hours were collected by pipette and transferred to glass cover slips in about 0.5 mL of sea water (SW). When tadpoles had attached the dish was flooded with SW which was then changed daily. In some cases, colonies that had triggered to the water surface were gently rotated and pressed to the glass surface. To increase contrast colonies were stained for 2 minutes with a 1:10 dilution of a 10 percent solution of Neutral Red and then washed 3 times in SW.

Microscopy and image collection

Growing colonies were observed using an Olympus SZX16 stereo microscope, typically with a 1x objective and a zoom setting of 1 to 4. Darkfield illumination from below was provided by the integrated LED ring. Images and video were recorded by an attached Canon Rebel 600D camera.

Image analysis software

Color MOV files were converted to greyscale image sequences with the Apple QuickTime Player 7 application. These images were scanned using a custom Java plugin for the NIH open-

source application ImageJ. The scanning strategy is a hybrid between human definition of the object to be scanned and the programmatic scanning of that object. Thus, the first step is to make a black mask, i.e., a solid black blob, that just fills the object to be scanned, e.g., one ampullae. The commercial software Photoshop was used to make this mask. This mask image is then inserted as the first frame in the image sequence to be scanned and it directs and defines scans of the remaining images.

The user picks a direction for the scan lines and a threshold to define the ends of chords across the target. The total number of pixels in all chords is the area. The ends of chords found during scanning are displayed superimposed on the actual image to enable the user to adjust thresholds etc. to obtain a good value for area, or in the extreme to just abandon the attempt to scan the image. This ability to curate the scanning process is essential to produce reliable data.

Heartbeats of the peristaltic heart were defined by periodic variations in grey levels over a small, e.g., 16-pixel, mask.

Image processing, mathematical analysis and graphical presentations were accomplished using the commercial software Photoshop™ and Mathematica™.

Results

The free-swimming larval form, or “tadpole”, of the tunicate B. *viocella* is released from its colony and swims for 1 to 3 days before attaching to a solid surface where it metamorphoses to the adult form as a filter feeder in approximately 24 hours. The larvae are large and complex compared to most other tunicates, and a heartbeat can be seen. The circulatory system is highly compressed at this stage and is further obscured by the tunic gel enclosing the tadpole. However, the approximately 30 ellipsoidal ampullae are visible as a parallel bundle around the surface of

the anterior. The ends of these ampullae will be the major regions of attachment to the solid substrate, after which the ampullae rapidly spread outward radially on the surface.

Even at the time of attachment several small buds can be seen on the surface of the tadpole. Each bud is developing into a new individual, or zooid, to augment the parental zooid in the growing colony. The time chosen in this report to document pulsations of the ampullae and other parts of the colony is a compromise between delaying long enough for the ampullae to be clearly visible as they spread out from under the zooid body, but before the zooid, buds, and the associated circulatory network grow and become even more complex. The exact number of ampullae, the pattern they form on the surface, the details of the connecting vessels, the size and number of zooid buds, and the periods of contractions vary from colony to colony. The first zooid of the colony is sometimes called the oozooid, to emphasize that it has developed directly from the egg. However, since only young colonies, which contain only an oozooid are considered here the distinction will be dropped for this report.

General conclusions made in this report have been distilled form observation of more than 100 colonies over two years. However, the majority of actual measurements presented in the Figures come from one colony that had a combination of characteristics that facilitated observation and quantitative measurement. The focus on one colony reveals how all its parts function together. The non-random complex morphological variations from one colony to the next and the chaotic variations in motion over time make most simple arithmetic statistics, e.g., averages, of limited use.

A typical tunicate colony

The colony seen in Fig. 1 was initiated 4 days earlier by a 1-day old tadpole. This grey level image was derived from one frame of a color video sequence of 2048 seconds. The area of ampullae number 1 was obtained by a computer-controlled scan documented in the insert and described in detail in in the Methods section. The solid white lines in the insert are the ends of chords that define the area.

The vessel network connecting ampullae and zooid

The vessel network that links the ampullae and zooid can only be partially discerned in Fig. 1. In order to obtain a more detailed and functional description the contrast was greatly increased using software and blood cell movement was visualized by repeated examination of accelerated (time-lapse) segments of the video.

The resulting map of functional vasculature is presented in Fig. 2. as a net of red lines that for the most part overlay the sometimes-faint grey lines seen in Fig 1. There are also small ampullae that may grow into larger ones, but their behavior is not described in this report. The basic topology of the net is a set of radial vessels from ampullae to a vessel ring which appears here to be connected to the zooid body at only 5 locations, but the central segment of the network is obscured by blood movement in the zooid body. Previous observations indicated that typically these vessels connect to circulation in the zooid or associated buds at 2-4 locations. Note that a few ampullae are almost directly connected to each other, e.g., 20 and 21, while others are far more isolated, e.g., 15 and 16.

Contractions of one ampullae

Contractions of ampullae diameters along the tip-base axis are generally in phase, which was the case for all the ampullae that could be reliably scanned in the colony seen in Figure 1.

However, for some ampullae in some colonies, contraction of some segments (a few percent of the total), can be significantly out of phase. Thus, the mechanism of contraction does not absolutely ensure synchrony in all ampullae.

As seen in Figs. 1 and 2 the two-dimensional profiles of most ampullae appear to approximate an ellipse with a length about 2-4 times longer than the width. Observation of accelerated videos suggested that width changes more than length during the rhythmic pulsations and measurement confirms this conclusion.

Actual measurements of changes in width and length of amp 1 over a period of 1024 seconds are seen in Fig. 4. Though the ampullae's width is only about 1/3 its length, the width changes by about twice the absolute number of pixels. Changes in the widths of ampullae 1, 19, and 25 were found to have a range of 37, 27, and 23 percent, while the lengths had a range of 7.5, 5.3, and 8.7 percent respectively. Thus, rather than being similar to elastic balloons that expand and contract symmetrically, ampullae are more like elastic cylinders that expand and contract mostly in radius. One consequence of this asymmetry is that the measured changes in area of the profiles are fair approximations to changes in the surface area of the ampullae.

Figure 5 is a plot of the contraction profile of ampullae 1 for 2048 seconds and for comparison a sine wave picked by eye to match the regular parts of the ampullae curve as best as possible. This sin wave has 25 cycles in 2048 seconds, thus a period of 82 seconds. The average period of ampullae contractions in 12 other colonies was found to vary from 62 to 143 seconds, with a mean of 104 seconds, thus the period of the colony seen in Fig. 1 is fairly typical. While the contractions of ampullae 1 are similar to the sine wave in many segments the ampullae peak time differences are not constant, peak shapes change, and peak extremes are not all the same.

An intuitive way to characterize an oscillating curve is to measure the times between the maxima, the peak-to-peak times. The average peak to peak time for ampullae 1 is 76 seconds, quite close to the constant 82 second peak to peak time of the sine wave, but the standard deviation of the ampullae times is 22 percent, because ampullae peaks often come slightly before or after the peaks of the sine wave.

One quantitative comparison between the contractions and sine waves is obtained by computing the Fourier power spectrum (FPS), seen in Fig. 6, which is sensitive to peak times, heights, and shapes. The major peak for ampullae 1, at a frequency of 26 per 2048 seconds (period of 79 seconds) is only 15.9 percent of its total power, with the remaining distributed over many higher and lower frequencies. As expected, (or defined) the power spectrum of the sine wave with that frequency has but a single peak containing 100 percent of the power at this frequency.

Contractions of a group of ampullae

To see variation and search for patterns of similarity between contractions of many ampullae with respect to both position and time we need to be able to see a lot of data in one graphic, but not with great precision. Coding ampullae areas as colors makes this possible. The areas of 15 adjacent ampullae, more than half the colony perimeter, over a time span of 2048 seconds are seen in Fig. 7 as 15 parallel vertical time lanes, with yellow representing large, green average, and blue small areas.

Ampullae 14 and 15 have similar patterns. Ampullae 20 and 21are seen to share many dramatic blue bands, for example at 200, 1050, 1200, 1570, 1800 and 1950 seconds. This is not surprising since each of these pairs are neighbors connected by a short vessel segments as seen in

Fig. 2. Ampullae 16, 17, and 18 have similar large peaks for the first 800 seconds, but share some, but not all, blue bands after that. Lanes 9 and 10 share many bands. In general, neighboring ampullae tend to be similar, and distant ones different.

However, the lack of a simple or even symmetric relation between contractions of most ampullae is consistent with the complex and mostly non-symmetric geometry of the vessel net connecting the ampullae with each other and the zooid. It is interesting that adjacent segments of distinct peak patterns do not seem to "diffuse" laterally to neighboring ampullae, they just come and go in their own neighborhood.

The periodicity of each of the 15 ampullae can be assessed in Fig. 8, a color map of their Fourier power spectra. The total power in the spectra displayed in this map have not been normalized for each ampullae, thus ampullae that have more extreme contractions have higher total values over all the frequencies. This is illustrated by more red in lane 21 compared to lane 9. The considerable differences between ampullae are clear.

Correlations between pairs of ampullae

Only an intuitive feeling for correlations of contractions between the 15 ampullae can be obtained by examination of Figs. 7 and 8. In contrast the actual values of all the possible 105 pair wise correlations of contractions are represented as colors in Fig. 9. Three red 2x2 squares along the diameter of Fig. 9 indicate the high correlations between the ampulla 10-11 pair, the 14-15 pair, and the 20-21 pair. In contrast, the blue rectangles toward the upper right and lower left corners represent the high negative correlation between the 20-21 pair with ampullae 8 through 12. Ampullae that are neighbors are more likely to be correlated than pairs that are distant, but the detailed pattern is complex, and any other generalization is not obvious.

Rolling time correlations between ampullae

A rolling time (time windowed) correlation between two sequences is a series of correlations between two small subsets of the sequences that moves along in time. It thus reveals transient time dependent correlations that are averaged out when the entire series are compared.

Figure 10 displays the rolling time correlation between ampullae 11 and 12. The two ampullae are highly correlated in a 60 second window for the first 900 seconds, then become much less for 100 seconds, then return to high correlation for another 500 seconds. The remainder of the time they abruptly go into and out of correlation several times. A sequence of periods of almost complete and low correlation is characteristic of two oscillators that are partially entrained.

Phase portraits of two ampullae

The phase portrait, showing the trajectory of an object's motion, in phase space, is a common tool used to understand dynamical systems. It can reveal subtle aspects of a system and is not linked to a specific function, as Fourier analysis is. The top panel of Fig. 11 shows the plot of area versus time for ampullae 9, with the brown segment indicating the segment to be plotted as a phase portrait in the lower panel. The curve displayed there, starting with the green and ending with the red segment, is the ampullae area versus the time derivative of that area. If a time axis where to extend upward from the paper, this curve would be a helical trajectory. In this Figure it is collapsed on the plane of the page.

The trajectory for a pure sine wave would be a series of superimposed ellipses, one for each complete cycle of the wave. If the area of the ampullae was suddenly altered by an external force, but the system was stable, the trajectory would leave the ellipse but then gradually return to the original elliptical curve, which is thus called an attractor. In contrast, the trajectory for

ampullae 9 is a series of loops of increasing size reflecting the increasing size of the cycles in the top panel. The trajectory is flat on the left (most negative values of area) because the derivative changes a great deal over a small range of area, the actual data curves are sharper on the bottom. A model for ampullae 9 would be an oscillator with an intrinsic frequency being influenced by modest, gradually increasing external forces causing excursions from the intrinsic ellipse.

The trajectory for ampullae 21 over the same time period, seen in the bottom panel of Fig. 12, is quite different, a reflection the different pattern of the raw date seen in the upper panel. Three of the trajectory loops have small subloops or extrusions. These correspond to small inflections or peaks in the data. Thus, strong but transient forces are modulating the behavior of this ampullae.

Vessels connecting ampullae also contract

Observation of time lapse versions of videos of colonies revealed that the widths of all vessels connecting the ampullae and zooid body were contracting along with ampullae contractions. A scan of a vessel near an ampullae, seen in Fig. 14, confirmed and measured these contractions. In fact, the percent change in the vessel width is perhaps slightly larger than the change in ampullae area for this specific region.

The sum effect of all ampullae in the colony

Since most ampullae are not always in complete synchrony, the sum effect of the contractions, pumping blood in and out of the zooid body, should be less than maximal because some flow will just be from one ampullae to another. It was possible to scan 19 of the 27, ampullae, with good sampling around the periphery of the colony. The sum of all 19 was a curve very similar to that seen previously for individual ampullae, with a range of 19.1 percent from the mean.

However, the mean of the range of individual ampullae was 30.5 percent. Thus, lack of complete synchronization has reduced net pumping to 63 percent of the possible maximum.

The zooid body and its peristaltic heart

In preceding sections, it has been shown that contractions of the ampullae and associated vessels are sufficiently synchronous to produce a net flow in and out of the zooid body with a period of about 80 seconds for this colony. This flow must cause parts of the zooid to swell and contract with the same period but opposite phase. However, the zooid is not a solid mass of tissue, rather it can be approximated as a small posterior region containing viscera plus two large concentric cylinders enclosing sea water. The outer cylinder is the body wall and the inner cylinder the brachial basket that supports the mucus feeding net. Thus, while some portion of the body must expand and contract, all that is clearly visible in the videos is the outer profile of the zooid. However, measurement of the area of this outer profile shows that in fact it does contract rhythmically with the same frequency but mostly 180 degrees out of phase with ampullae contractions, as seen in Fig 14.

A peristaltic heart in the posterior region of the zooid body, with a beat rate approximately 100 times faster than contractions of the ampullae, circulates blood throughout the zooid. This heart periodically changes direction, which can be identified, in favorable cases, by viewing videos of a colony. In Fig. 15 the direction of blood flow generated by the peristaltic heart is represented by the rectangular curve alternating between 100 percent in the anterior direction along the endostyle, and 100 percent to the posterior. Contractions of the ampullae are superimposed for comparison. Starting at the left end of the graph it is possible to associate a minimum of the ampullae curve with a heart flow transition across most of the graph. Thus, in

this colony, flow due to the peristaltic heart appears to be entrained with flow due to ampullae contractions, but with twice the period.

Contractions of a detached pair of ampullae.

In 1899 Frank W. Bancroft published observations on contractions of ampullae of colonial tunicates in an report (Bancroft 1899) that is quite accessible today since it has been reprinted. He also described contractions in groups of ampullae that had been surgically separated from colonies.

Fig. 16 describes the contractions of the most simple group, a pair. These detached ampullae were connected to each other by a short vessel segment, similar to that seen between ampullae 20 and 21 in Fig. 2, however they came from a different colony. The uniformity and symmetry in these pair of contractions is apparent to the eye. The average of the peak-to-peak times was 127 seconds, with a standard deviation of 9.4 percent. The curves are almost indistinguishable from sine waves, with 94 percent of the total power spectrum in the main frequency.

Contractions of single detached ampullae

Even single detached ampullae contract with periods similar to those observed when they were attached to a colony. While the total volume can't change in one isolated ampullae because blood is incompressible, the ampullae can and does oscillate as can be seen by blood cell movement and by changes in shape as documented in Fig 17.

In all ampullae described in this report changes in shape or size were correlated with movement of blood cells. If ampullae are part of a colony blood cells move in or out of the ampullae, in a detached pair blood cells move from one ampullae to the other; in detached single ampullae blood cells move from one end to the other. Blood cell movement is usually the only

way to see changes in shape or size when viewing in real time with a microscope because changes in shape and size are too slow for the human to perceive directly.

The image of a single detached ampullae, the fifth in a series of 6, is seen in the upper left panel of Fig. 17. A segment of this and a another ampullae in the series were scanned and the results are presented in the middle panel. Note that there is nothing fundamental about this segment, it was chosen merely because it changed the most, other ampullae change shapes in different patterns.

The time course of contractions of the series of 6 were followed for approximately 1000 seconds. In contrast to previous Figures, only the times of peaks have a simple meaning. The means and standard deviations of peak-peak times are seen in Table 1 and the curves for ampullae 1 and 5 are presented in the lower panel of Fig. 17.

The first and fifth ampullae seem so similar as to invite a comparison. Thus, the first peak of each was aligned and the two plotted together to make the bottom panel of Fig. 17. While the peak heights of each of the two ampullae change with time and pattern, the peak times match up to an amazing extent, with the 14^{th} peak of both matching within 3 seconds out of the total of almost 900.

Discussion

Summary of results

This report presents area versus time profiles from images of different parts of the colonial tunicate *B. viocella* and documents their rhythmical contractions. In the first section a single colony is observed over a period of 2048 seconds. The ampullae contract and expand, often in synchrony with each other and with contractions of the network of vessels connecting them to

the zooid. These results are consistent with qualitative observations made by Mukai et al. (Mukai et al. 1978).

Fourier power spectra of different ampullae have a variable fraction, but always less than half, in the main frequency. Phase portraits of contractions of some ampullae are almost circular, consistent with sinusoidal contractions, while portraits of others show complex chaotic behavior. Rolling correlation plots of neighboring ampullae pairs show that they transition from periods of being highly correlated to uncorrelated and back. Thus, correlations over the full 2048 second period are a time average of being in and out of synchrony, and not a constant intermediate value.

The sum of contraction profiles of half of the ampullae of the colony is a semi-sinusoidal curve with a range about half as large as individual ampullae, and thus there must be net flow of blood in and out of the zooid body. The body is not a solid mass of tissue, but mostly cylindrical space containing sea water, thus it need not change its external shape due to this flow. However, it does contract and expand, 180 degrees out of phase with the ampullae.

Blood is circulated throughout the body by a peristaltic heart which reverses direction about every 100 seconds. In the tunicate studied here these heart reversals are mostly correlated with ampullae contraction in a 1:2 pattern, i.e., when the ampullae contractions are maximal the heart changes direction, and thus the two appear to be entrained.

It has been known for more than a hundred years that groups of ampullae surgically detached from the colony continue to contract (Bancroft 1899). Thus, contraction is an intrinsic activity of ampullae. In the present study pairs of detached ampullae connected by a short vessel contract with much greater regularity than the ampullae in colonies. The time profile of contractions of these pairs is indistinguishable from two sine waves 180 degrees out of phase.

Single detached ampullae also oscilate, with a period similar to those when they were part of a colony, but with different shapes, because the volume of each ampullae must remain constant. Thus, only the times between peak values can be compared to connected ampullae. Periods of six neighboring detached ampullae were found to be remarkable similar, which could be the result of entrainment.

It is proposed that the irregularity of contraction patterns of the large number of ampullae in a colony is due to weak interactions with neighbors with very similar but not identical periods. Since these are independent oscillators which fall in and out of synchrony with their neighbors, it can been seen as an example of entrainment (Ermentrout & Rinzel 1984).

Entrainment and chaos

Entrainment is the synchronization of independent oscillating or rotating units by exchanges of modest energy compared to the total of the system (Pantaleone 2002; Willms et al. 2017). Entrainment is different from a cause-and-effect relationship such as the engine and propeller of a ship, and quantitatively different from an effectively deterministic phase lock involving large amounts of energy, as can be the case for generators on a common electrical grid.

Neighboring ampullae tend to have contraction profiles that are more correlated while those more separated, for example on opposite sides of the colony, have less correlated profiles. Ampullae connected by short vessel segments tend to have more correlated contractions than those connected by longer segments. Thus, the highly visible hydraulic connection between ampullae might be the major linkage between them. However, while to the eye ampullae look like pods, and vessels look like tubes, in reality they are ellipsoidal and cylindrical cavities in the tunic, coated on the inside by a thin layer of epithelial cells. Thus, when ampullae and vessels

contract, the tunic in which they are embedded contracts, with resulting mechanical strain transmitted to all parts of the colony in some proportion to proximity. If contraction is the result of action-myosin muscle, synchronization of cells in each ampullae is likely to involve waves of electrical depolarization moving across walls of the ampullae, mediated by gap junctions between cells, and might well bleed over to neighboring ampullae. Thus, hydrolytic forces, mechanical strain and electrical fields could all be part of the entraining mechanism.

A dynamic system is said to be chaotic if there is no obvious repeating pattern and thus the motion cannot be predicted. In the ampullae system there is an obvious common frequency of contraction for all ampullae, but the occasional shifts in frequency, phase, and amplitudes appear to have no simple pattern. A chaotic system can still be deterministic, described by equations, perhaps complex, that have unique numerical solutions when the initial conditions are known with infinite accuracy. However, since the tunicate colony is growing, and thus changing its geometry at a rate comparable to the possible repeats of the contraction pattern, actual repeatability may never occur.

Does entrainment benefit the tunicate?

Ampullae and attached vessels are composed of cells, and cells need glucose for energy and substrates for biosynthesis and repair, e.g., amino acids. The only sources for these nutrients are the stomach and intestine in the body of the tunicate, and they must be transported by blood flow. The peristaltic heart that distributes blood by circulation through the body cannot pump blood through ampullae, which must rely on the reciprocal flow their contractions provide. If contractions of ampullae were completely uncorrelated with each other the net pumping effect

would be much less than if they were completely synchronized, since much of the flow would be between ampullae and not between the ampullae and the zooid body.

Some of the previous Figs. show contractions profiles of different ampullae that are essentially identical for many contraction cycles, while others are very different for at least several cycles. The mean of the ranges of projected areas of the 15 individual ampullae described in Figs. 7-9 for the 2048 second time period are 31 percent, while the range of the sum of the 15 ampullae during that same time period is 17 percent. Thus, as expected, the range for the sum is lower than expected if synchronization were complete. Only half of the ampullae were analyzed in the Figs. mentioned, and the difference between the observed range of the sum and individuals would be expected to be larger if all ampullae had been followed.

If each of 15 ampullae had sinusoidal contraction curves of the same amplitude and frequency, and ranged between +1 and -1, and were completely synchronized, the sum would range between -15 and +15, for a total range of 30. If instead each of the 15 had a random phase difference from its neighbors, the mean range in a simulation with 1000 different combinations of random phase differences had a total range of 6.7, about 4.5-fold lower than if completely synchronized. These calculations suggest that the tunicate achieves about half the possible benefit of complete synchrony.

The out of phase contraction of the zooid body is not surprising, blood expelled from the ampullae must cause some part of the zooid body to expand, thus it may be more cause and effect than entrainment. It’s impossible to determine the fraction or even the sign of the work of pumping done by the body just by observation; active body contraction may not occur, and if it does it could oppose or enhance ampullae contraction. The outer body wall of tunicates certainly

possesses muscle, and tunicates often expel a large fraction of the enclosed water when an irritating object is drawn into the feeding basket; they are sea squirts after all.

The mechanism of entrainment of the peristaltic heart with ampullae is not obvious. However, one would guess that when ampullae pump blood into the zooid body it could create a higher pressure at one end of the peristaltic heart tube than the other.

Toward a molecular model

The cellular walls of external vessels are a single layer, as are capillaries of vertebrates, but the tunicate vessel diameter of 20 to 50 microns is more similar to the small arterioles and veins that supply and drain blood from capillaries. However, since blood flow reverses on average every 100 seconds there can be no arterial-venous asymmetry. The innermost layer of vertebrate vessels is endothelial, with a basement membrane on the outside, while the tunicate vessel wall in epithelial in nature, with what appears to be a basement membrane on the inside, next to blood flow (Rodriguez et al. 2019).

There are vascular systems in vertebrates that contract rhythmically, e.g. the myoepithelial cells in the ducts of the mammary gland and lymphatic vessels (for an overview see (Hashitani & Lang 2019)). However, vertebrate blood vessels that contract have an outer layer of muscle cells, with actin-myosin sarcomere fibers containing periodic bands that are conspicuous in the electron microscope. No sarcomere bands are seen in EM pictures of the external tunicate vessels.

Muscle contractions are produced by voltage pulses, action potentials, which have been reported to occur on the external vessel walls of *Botryllus* (Mackie 1995; Mackie & Singla 1983). However, in the published figures the sharp voltage pulses last for about a second and occurred

418 at most once during each complete contraction cycle. In vertebrate systems muscle contraction
419 starts shortly after the beginning of the voltage pulse and ends within 1-2 times the length of the
420 pulse (Wooderchak-Donahue et al. 2013). In order to produce contractions with periods of about
421 100 seconds, one would thus expect at least tens of action potentials separated by increasing and
422 the decreasing time intervals during the contraction cycle.
423 A more likely source of tunicate vessel contractions are stress fibers, 4-9 nm diameter electron
424 dense microfilament bundles (De Santo & Dudley 1969; Katow & Watanabe 1978; Simon-
425 Blecher et al. 2006; Torrence & Cloney 1981) which stain using the fluorescent dye labeled
426 palladium, a mushroom toxin which binds specifically to actin (Madhu et al. 2020; Rodriguez et
427 al. 2021). Intrinsic rhymical motion is seen in angiogenesis of blood vessels in vertebrates
428 (Ehrmann et al. 2019), where stress fiber contraction powers side-to-side searching of the
429 growing tip of blood vessels in the process of migrating up a chemical gradient, e.g. vascular
430 endothelial growth factor (VGF) (Yokota et al. 2015). The growth cones at the tips of vertebrate
431 axons oscillate in a similar way (Sakumura et al. 2005) and extension of the leading edge of
432 migrating fibroblasts extend and contract (Pertz 2010) as they move across a surface. The
433 monolayered epithelium of the *Drosophila* gastrula elongates during development not by a
434 smooth process but by a series of discrete expansions (Loerke & Blankenship 2020; Martin
435 2010). All these processes have periods of about 100 seconds, similar to the contractions of
436 ampullae.
437 These actin contractions are controlled by small RhoGTPases with activities modulated by a
438 large, at least 145 types in man (Muller & al. 2020). The GTPases in term are controlled by a
439 group of GTPase activators, GTPase exchange factors, and GTPase inhibitors, which can inhibit
440 or stimulate each other to form an oscillating network (Bolado-Carrancio et al. 2020; Ehrmann et

al. 2019; Sakumura et al. 2005). A large number of these GTPase associated proteins are found in the tunicates that have been studied (Fort 2018; Philips et al. 2003) .

The activity of these GTPases can be modulated by mechanical tension at cell-cell cadherin structures, as summarized in a review chapter by Monaghan-Benson and Guilluy (Monaghan-Bensen & Guilluy 2018), and cell-matrix integrin junctions (Tulla et al. 2007). Thus, contractions of cells comprising the ampullae and vessel walls could be but one example of a widly distributed family of oscillators, generated and synchronized by mechanical forces, no electricity required.

Toward a mathematical model

The tunicate colony is a dynamic system, a collection of oscillating, interacting components, evolving with time. Description of such a system entails a mathematical model, which would start with a description of individual ampullae. The simplest system with trans-ampullae flow is a pair of connected ampullae, which has been shown here to oscillate as two, out of phase, sine waves.

Systems of coupled oscillators play important roles in biology, physics, and engineering and have been of considerable interest to applied mathematicians for some time. For an important class of such systems, coupling between i oscillators, with intrinsic frequencies ω_i, primarily effects the phases, θ_i, the amplitudes remaining constant. These systems are thus often represented shown as points moving around the unit circle, instead of a graph of amplitude versus time as seen in the Figures of this report.

$$a_i = \sin(\omega_i t + \theta_i) \quad (1)$$

A seminal publication in 1975 by Kuramoto (Kuramoto 1975) presented a simple equation describing the behavior of a collection of N interacting oscillators with a symmetrical distribution of intrinsic frequencies, ω_i, but interactions of each with all others characterized by the single factor λ.

$$\dot{\theta}_\iota = \omega_i + \frac{\lambda}{\mathrm{N}} \sum_{j=1}^{N} \sin(\theta_i + \theta_j) \quad (2)$$

This equation has sufficient application that demonstrations of numerical solutions using commercial computational software are available on the Internet, e.g. Mathematica (Alfonsi 2016).

A single interaction coefficient between all ampullae would not be compatible with data presented here, while a single intrinsic frequency of oscillation, unlike the distribution of frequencies in (2), is quite plausible. In addition, while the oscillators described in (2) do synchronize to a single ω for sufficiently large λ and time, the phases do not become equal, i.e. lock, while actual tunica ampullae do spend a significant fraction of time with locked phases.

However, the Kuramoto equation is important not because it accurately describes all coupled oscillator systems, rather because it has been the seed for a profusion of related models. A history of some of these developments has been presented by Strogatz (Strogatz 2000), and a comprehensive review of theories of complex oscillator networks has recently been published by Rodrigues et al. (Rodrigues et al. 2016). To model ampullae contractions, the addition of a second order derivative provides “inertia”, so phases will lock (2):

$$\ddot{\theta}_i = -\alpha\,\dot{\theta}_i + \omega_i + \frac{\lambda}{\mathrm{N}}\sum_{j=1}^{N}\sin(\theta_i + \theta_j) \quad (3)$$

When interactions between the oscillators are weak, or the distribution of intrinsic frequencies is broad, oscillators will lock in and fall out of synchrony to the mean with a pattern that has no obvious pattern, at least over a "short" time period, which actually may be very long. In this case the system is said to be chaotic, as described in the previous section. As an example, in the first lane of Fig. 7 describing ampullae 8, there is a series of peaks with high values in the first 600 seconds, but no similar behavior in the remaining 1500; what is the average pattern? In some systems you can observe almost arbitrarily long times and thus see complex patterns. However, significant growth and change in colony morphology occurs in a time span only slightly longer than that covered in Fig. 7, thus precluding likely observation of rare events.

However, the Kuramoto approach of considering the ampullae as a collection of oscillators implies the system can be described using only the phases of the oscillators, while many of the ampullae exhibit very different peak values. Thus the ampullae system may require a more complex model.

Quick and easy

The data graphed in this report was analyzed using a computer and both custom and commercial software. Some investigations do require careful quantitative analysis, but many qualitative conclusions can be made intuitively in seconds only using video viewers that are included with both Microsoft and Apple operating systems for personal computers. The major difficulty in observing ampullae behavior is that it is slow; it's like trying to see a plant grow. This can be overcome by using the slider in a video viewer. Typically, the viewer is allowed to run at the

native speed, 30 frames per second, and the slider moves across the underside of the video window to indicate the fraction that has been observed. However, if you grab the slider with the mouse and pull or push it along its track, the video plays at the corresponding speed; it's generating a time lapse movie on the fly. Once this author discovered this technique it was always used on video files before a more methodical analysis. As any scientist knows, it is much easier to design a protocol if you know the answer. One wonders how much movement in biological systems has not been noticed just because of a speed mismatch between observer and observed.

Conclusions

Measurement of the profiles of more than half of the 27 ampullae around the periphery of a young tunicate colony for 2000 seconds documents rhymical contractions with periods of about 80 seconds. Contractions of some colonies are quite regular in shape and timing while those of others are less so. However, in no instance is more than 50 percent of the energy in the Fourier power spectrum in the main peak. Contractions in neighboring ampullae on the periphery tend to be more correlated than those on the opposite side. Contractions in each ampullae tend to have regular timing for a time segment, then become very irregular, then snap back to regular timing. However, pairs and single ampullae surgically detached from the colony typically beat with extremely regular, constant periods and wave shapes, typically having 99 percent of the power in the main peak of the Fourier spectrum. This fact is consistent with the ampullae in a colony contracting independently with approximately equal internal timing, but mostly entrained in phase by the connecting net of blood vessels. Entrainment provides a greater reciprocal exchange of blood between the ampullae and the zooid body than would occur with randomly timed

contractions. The cells in the ampullae and associated vessel net depend on nutrients from the digestive system of the zooid, and nutrients must be transported by ampullae contractions. The peristaltic heart in the zooid body reverses pumping direction at times mostly correlated with ampullae contractions. This may also increase ampullae-body blood transfer.

Data Availability

Code of the Java plugins for ImageJ used in this report to scan video frames and measure areas of ampullae etc. can be obtained at http://doi.org/10.5281/zenodo.6114322. The raw data from these scans can be obtained at the same location. The author will honor reasonable requests for additional data.

References

Alfonsi J. 2016. Kuromoto model for phase locking of coupled oscillators. p http://demonstrations.wolfram.com/KuramotoModelForPhaseLockingOfCoupledOscillators/.

Bancroft PW. 1899. A new function of the vascular ampullae in the Botryllidae. *Zoologischen Anzeiger* 13:450-462.

Bolado-Carrancio A, Rukhlenko OS, Nikonova E, Tsyganov MA, Wheeler A, Garccia-Munoz A, Kolch W, von Kriegsheim A, and Kholodenkod BN. 2020. Periodic propagating waves coordinate RhoGTPase network dynamics at the leding and trailing edges duriing cell migration. *eLIFE* 9:e58165.

De Santo RS, and Dudley PL. 1969. Ultramicroscopic filaments in the ascidian Botryllus schlosseri (pallas) and their possible role in ampullar contractions. *J Ultrastruct Res* 28:259-274.

Ehrmann A, N'guyen B, and Seifert U. 2019. Interlinked GTPase cascaded provide a motif for both robust switches and oscillators. *Interface* 16:20190198.

Ermentrout GB, and Rinzel J. 1984. Beyond a pacemaker's entrainment limit: phase walk-through. *Am J Physiol* 246:R102-R106.

Fort P. 2018. Rho signaling: an historical and evolutionary perspective. In: Fort P, and Blangy A, eds. *Rho GTPases Molecular biology in health and disease*. New Jersey: World Scientific, 3-18.

Gasparini F, Manni L, Cima F, and al. e. 2014. Sexual and Asexual Reproduction in the Colonial Ascidian Botryllus schlosseri. *Genesis* 53:105-120.

Hashitani H, and Lang RJ. 2019. Smooth muscle spontaneous activity. Physiological and pathological modulation. Singapore: Springer.

569 Katow H, and Watanabe H. 1978. Fine structure and possible role of ampullae on tunic supply
570 and attachment in a compound ascidian, Botryllus primigenus OKA. *J Ultrastruct Res*
571 64:23-34.
572 Kuramoto Y. 1975. Self-entrainment of a population of coupled non-linear oscillators.
573 International symposium on mathematical problems in theoretical physics. Heidelbert:
574 Springer.
575 Loerke D, and Blankenship JT. 2020. Viscoelastic voyages- biophysical perspectives on cell
576 intercalation during *Drosophila* gastrulation. *Semin Cell Dev Biol* 100:212-222.
577 Mackie GO. 1995. Unconventional signalling in tunicates. *Mar Fresh Behav Physiol* 26:197-205.
578 Mackie GO, and Singla CL. 1983. Coordination of compound ascidians by epithelial conduction
579 in the colonial blood vessels. *Biol Bull* 165:209-220.
580 Madhu R, Rodriguez D, Guik C, Shambhavi S, De Tomaso AW, Valentine MT, and Loerke D.
581 2020. Characterizing the cellular architecture of dynamically remodeling vascular tissue
582 using 3-D image analysis and virtual reconstruction. *Mol Biol Cell* 31:1714-1725.
583 Manni L, Gasparini F, Hotta K, Ishizuka KJ, Ricci L, Tiozzo S, Voskoboynik A, and Dauga D.
584 2014. Ontology for the asexual development and anatomy of the colonial chordate
585 Botryllus schlosseri. *PLoS ONE* 9:e96434. 10.1371/journal.pone.0096434
586 Manni L, Zaniolo G, Cima F, Burighel P, and Ballarin L. 2007. Botryllus schlosseri: a model
587 ascidian for the study of asexual reproduction. *Dev Dyn* 236:335-352.
588 10.1002/dvdy.21037
589 Martin AC. 2010. Pulsation and stabilization: contractile forces that underlie morphogenisis. *Dev*
590 *Biol* 341:114-125.
591 Monaghan-Bensen E, and Guilluy C. 2018. Rho signaliing in mechanotransduction. In: Fort P,
592 and Blangy A, eds. *Rho GTPases Molecular biology in health and disease*. Singapore:
593 World Scientific Publishing Co., 81-96.
594 Mukai H, Sugimoto K, and Taneda Y. 1978. Comparative Studies on the Circulatory System of
595 the Coumpound Ascidians, *Botryllus*, *Botrylloides,* and *Symplegma*. *J Morphol* 157:49-
596 78.
597 Muller PM, and al. e. 2020. Systems analysis of RhoGEF and RhoGAP regulatory proteins
598 reveals spactially organized RAC1 signalling from integrin adhesions. *Nature Cell Biol*
599 22:598-511.
600 Pantaleone J. 2002. Synchronization of metronomes. *Am J physics* 70:992-1000.
601 Pertz O. 2010. Spatio-temporal Rho GTPase signaling - where are we now? *J Cell Sci*
602 123:1841-1850.
603 Philips A, Blein M, Robert A, Chambon JP, Baghdiguian S, Weill M, and Fort P. 2003. Ascidians
604 as a vertebrate-like model organism for physiological studies of Rho GTPase signaling.
605 *Biol Cell* 95:295-302.
606 Rodrigues FA, Peron TKD, Ji P, and Kurths J. 2016. The Kuramoto model in complex networks.
607 *Physics Reports* 610:1-98.
608 Rodriguez D, A TD, Roopa M, Kassmer S, Loeke D, Valentine MT, and De Tomaso AW. 2021.
609 Vascular aging in the invertebrate Chordate, Botryllus schlosseri. *Fronteirs Mol Biosci* 8.
610 Rodriguez D, N'ourizadeh S, and De Tomaso AW. 2019. The biology of the extracorporeal
611 vasculature of Botryllus schlosseri. *Dev Biol* 448:309-319.
612 Rosental B, Kowarsky M, Seita J, Corey D, Ishizuka KJ, Palmeri KJ, Chen S-Y, Sinha R,
613 Okamoto J, Mantalas G, Manni L, Raveh T, Cllarke DN, Tsai JM, Newman AM, Neff NF,
614 Nolan GP, Quake SR, Weissman IL, and Voskoboynik A. 2018. Complex mammalian-
615 like haematopoietic system found in a colonial chordate. *Nature* 564:425-429.
616 Sakumura Y, Tsukada Y, Yamammoto N, and Ishii S. 2005. A molecular model for axon
617 guidance based on cross talk between Rho GTPases. *Biophys J* 89:812-822.

Simon-Blecher, Hanania J, Achituv Y, and Rinkevich B. 2006. Fine structure of naive and allogeneic challenged ampullae in Botrylloides subpopulation I from the Mediterranean coast of Israel. *Marine Biol* 148:978-996.

Strogatz SH. 2000. From Kuramoto to Crawford: exploring the onset of synchronization in populations of coupled oscillators. *Physica D* 143:1-20.

Tiozzo S, **Vkoskoboynik A**, **Brown FD**, and **Tomaso D**. 2008. A conserved role of the VEGF pathway in angiogenesis of an ectidermally-derived vasculature. *Dev Biol* 315:243-255.

Torrence SA, and Cloney RA. 1981. Rhythmic contractions of the ampullar epidermis during metamorphosis of the ascidian Molgula occidentalis. *Cell Tissue Res* 216:293-312.

Tulla M, Huhtala M, Jaalinoja J, Kapyla J, Farndale RW, Ala-Kokko L, Johnson MS, and Heino J. 2007. Analysis of an ascidian integrin provides new insight into early evolution of collagen recognition. *FEBS Lett* 581:2434-2440. 10.1016/j.febslet.2007.04.054

Willms AR, Kitanov PM, and Langford W. 2017. Huygens' clocks revisited. *R Soc open sci* 4:170777.

Wooderchak-Donahue WL, McDonald J, O'Fallon B, Upton PD, Li W, Roman BL, Young S, Plant P, Fulop GT, Langa C, Morrell NW, Botella LM, Bernabeu C, Stevenson DA, Runo JR, and Bayrak-Toydemir P. 2013. BMP9 mutations cause a vascular-anomaly syndrome with phenotypic overlap with hereditary hemorrhagic telangiectasia. *Am J Hum Genet* 93:530-537. 10.1016/j.ajhg.2013.07.004

Yokota Y, N'akajima H, Wakayama Y, Muto A, Kawakami K, Fukuhara S, and Mochizuki N. 2015. Endothelial Ca2+ oscillations reflect VEGFR signaling-regulated angiogenic capacity in vivo. *eLIFE*.

Figures

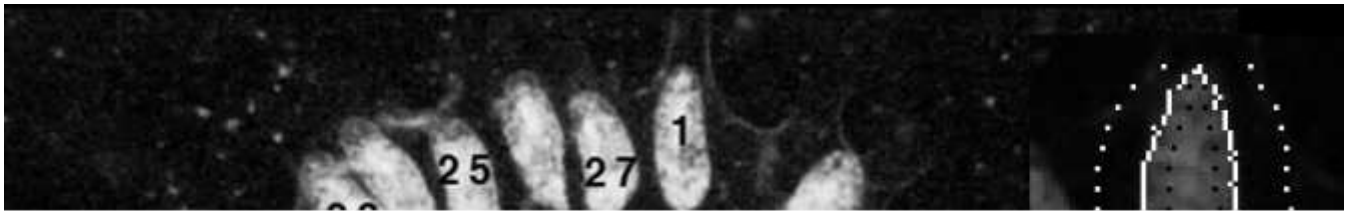

Figure 1

A typical young colony. Colonies were observed by dark field illumination and the image recorded by a video camera at 30 frames per second at a resolution of 640 by 480 pixels. This image is one frame from such a video with a field of view (FOV) of 5.6 x 4.2 mm; thus, the diameter of the colony is about 3.5 mm. An identification number was assigned to each ampullae in a clockwise direction around the colony. Areas of ampullae were determined as the sum of pixels in chords across the ampullae averaged over the 30 frames in each second of the video. Scanning of each ampullae was defined by a user generated mask and the results of scans of each ampullae were curated. The scan lines for ampullae number 1 were horizontal and are indicated in the insert enlargement where the size of individual pixels can be seen. The start and end of each scan chord are indicated by the rows of dashed white and black pixels while edges found between these limits during the scan are indicated by the two continuous rows of

white pixels. The thin white horizontal lines define upper and lower quarters of the ampullae. Scale bar at lower right = 1 mm.

Figure 2

The functional vessel network connecting ampullae and the zooid. Vessels (red) were identified by examination of high contrast images and blood cell movement in time-lapse sequences.

Figure 3

Contractions in segments of two ampullae. **Top panel;** ampullae 1 in Fig. 1, blue 2nd segment from tip, orange 3rd. **Bottom panel:** ampullae in another colony, blue tip segment, orange 3rd.

Figure 4

Width and length of ampullae 1 as percent of means. width in red, length in blue. The mean length was about 230 px or 2.0 mm and the mean width was about 75 px or 0.66 mm. The fractional change in width, or radius, of the ellipse is much greater than the change in length.

Figure 5

The contraction curve of ampullae 1 and a sine wave. amp in solid red, sine wave in dashed blue. Often the two curves are superimposable but occasionally ampullae peaks exhibit very different shapes and peak at different times.

Figure 6

The Fourier power spectrum of ampullae 6 contractions. amp isine wave

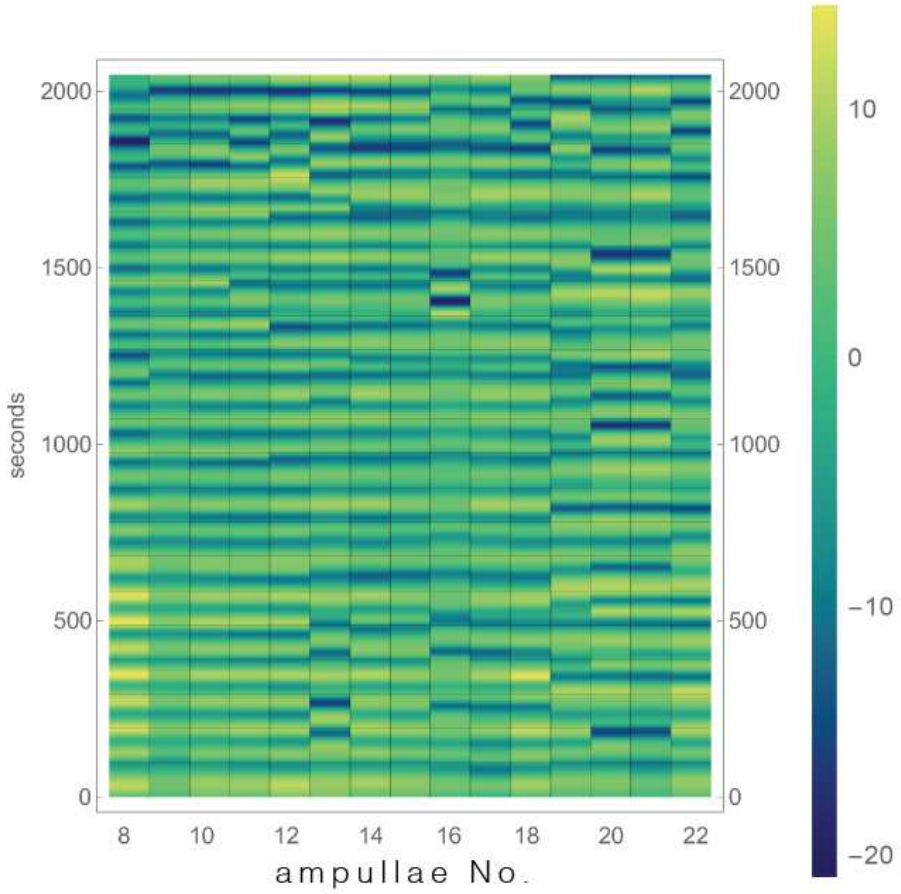

Figure 7

Percent differences in areas of 15 ampullae from their means over 2048 seconds. The indexes of the 15 ampullae are indicated along the bottom while time for each vertical lane increases from 0 to 2048 seconds moving up the lanes. The vertical legend bar on the right gives the relation between color and percent deviation from the mean value for each ampullae.

Figure 8

Terms of the Fourier power spectra for 15 ampullae are indicated by color. Lanes have not been normalized for totals of each ampullae, thus ampullae with more extreme contractions have more red cells. The legend bar on the left gives the relation between color and relative percent of total power.

Figure 9

Correlation of contractions between all possible pairs of 15 ampullae. The bar legend on the right gives the relation between correlation and color.

Figure 10

Contractions of ampullae 11 and 12 are seen in the top panel and the rolling time correlations between the two over successive 60 second periods are seen in the lower panel.

Figure 11

The phase projection of ampullae 9 over 400 seconds. The entire 2048 second profile is seen in the top panel, with the 400 second segment in brown. The phase projection in the lower panel has an arrowhead at the end of the segment. The area and its derivative have been normalized to percent of maximum range.

Figure 12

The phase projection of ampullae 21 over the same 400 second segment as

seen in Fig. 11.

Figure 13

Contractions of a vessel and its attached ampullae. vessel in blue, amp yellow. The vessel segment scanned was approximately 1/3rd the length of the ampullae and started this distance from the

ampullae-vessel junction.

Figure 14

Contractions of the zooid compared to ampullae. Zooid in blue, amp in yellow. The area of the zooid and the average of 19 out of the 27 ampullae of the colony seen in Fig 1.

Figure 15

Entrainment between ampullae contractions and reversals in the peristaltic heart. The top panel displays 14 beats of the peristaltic heart during a 12 second period, giving a period of 0.8 seconds. The beats were detected as variations in grey level in a video with no resolution of the structure of the heart. The bottom panel shows contractions of 12 ampullae in yellow and blood flow generated by the heart in blue, during 1200 seconds, 100 times the length of the top panel. During most of the 1200 seconds reversals of the heart occur at or near the maximum ampullae area, consistent with a 1:2 entrainment.

Figure 16

Contractions of a pair of detached ampullae. A pair of connected ampullae were surgically separated from a colony. **Top panel:** area versus time curves, trimmed to cross over times and normalized to percent of range. **Bottom panel:** Fourier Power Spectrum of blue line.

Figure 17

Contractions of single detached ampullae. The image of one detached ampullae is seen in the small upper left panel. The severed vessel that had connected the ampullae to the colony circulation is at the upper right end. A diagram in the small panel to the right displays outlines in blue and red of two most extreme shapes. Oscillations were observed by scanning a quarter of the ampullae, as indicated by the four arrows. The middle panel displays the results of such scans of ampullae 1 in blue and 5 yellow, in a consecutive series of 6 along the circumference of a colony. The time in seconds between each peak is plotted in the lower panel.

Supplementary Files

This is a list of supplementary files associated with this preprint. Click to download.

- Abbreviations.rtf
- SupplementaryInformation.rtf